Barrio, Rafael A.; Kaski, Kimmo K.; Haraldsson, Guđmundur G.; Aspelund, Thor; Govezensky, Tzipe

A model for social spreading of Covid-19

Published in:
Physica A: Statistical Mechanics and its Applications

DOI:
10.1016/j.physa.2021.126274

Published: 15/11/2021

Document Version
Publisher's PDF, also known as Version of record

Physica A 582 (2021) 126274

Contents lists available at ScienceDirect

Physica A

journal homepage: www.elsevier.com/locate/physa

A model for social spreading of Covid-19: Cases of Mexico, Finland and Iceland

Rafael A. Barrio [a,*], Kimmo K. Kaski [b,c], Guđmundur G. Haraldsson [d], Thor Aspelund [e,f], Tzipe Govezensky [g]

[a] *Instituto de Física, Universidad Nacional Autónoma de México, CDMX 01000, Mexico*
[b] *Department of Computer Science, Aalto University School of Science, Espoo, FI-00076, Finland*
[c] *The Alan Turing Institute, 96 Euston Rd, Kings Cross, London, NW1 2DB, UK*
[d] *Science Institute, University of Iceland, Dunhaga 3, Reykjavik, 107, Iceland*
[e] *Centre for Public Health Sciences, University of Iceland, Reykjavik, Iceland*
[f] *The Icelandic Heart Association, Reykjavik, Iceland*
[g] *Instituto de Investigaciones Biomédicas, Universidad Nacional Autónoma de México, CDMX, 04510, Mexico*

ARTICLE INFO

Article history:
Received 3 December 2020
Received in revised form 8 July 2021
Available online 17 July 2021

Keywords:
Pandemics
Epidemiological modelling
Stochastic processes
Non linear dynamics
Geographical spread
Social behaviour

ABSTRACT

The shocking severity of the Covid-19 pandemic has woken up an unprecedented interest and accelerated effort of the scientific community to model and forecast epidemic spreading to find ways to control it regionally and between regions. Here we present a model that in addition to describing the dynamics of epidemic spreading with the traditional compartmental approach takes into account the social behaviour of the population distributed over a geographical region. The region to be modelled is defined as a two-dimensional grid of cells, in which each cell is weighted with the population density. In each cell a compartmental SEIRS system of delay difference equations is used to simulate the local dynamics of the disease. The infections between cells are modelled by a network of connections, which could be terrestrial, between neighbouring cells, or long range, between cities by air, road or train traffic. In addition, since people make trips without apparent reason, noise is considered to account for them to carry contagion between two randomly chosen distant cells. Hence, there is a clear separation of the parameters related to the biological characteristics of the disease from the ones that represent the spatial spread of infections due to social behaviour. We demonstrate that these parameters provide sufficient information to trace the evolution of the pandemic in different situations. In order to show the predictive power of this kind of approach we have chosen three, in a number of ways different countries, Mexico, Finland and Iceland, in which the pandemics have followed different dynamic paths. Furthermore we find that our model seems quite capable of reproducing the path of the pandemic for months with few initial data. Unlike similar models, our model shows the emergence of multiple waves in the case when the disease becomes endemic.

1. Introduction

In today's globalised world people easily travel long distances to faraway places, where they can get infected, carry and consequently spread lethal and easily mutating viruses that could subsequently lead to wide-spread epidemic or

* Corresponding author.
E-mail address: barrio@fisica.unam.mx (R.A. Barrio).

https://doi.org/10.1016/j.physa.2021.126274
0378-4371/

even pandemic of catastrophic proportions. This causes a lot of concern among general public and huge strain in national healthcare and hospital capacities including their Intensive Care Units (ICUs), but also among public authorities and governments as to what measures, restrictions, recommendations to put in place and when, to keep the society running in balance with the rest of its socioeconomic functions.

The commonly accepted measures to counter the effect of air transmitted infections are recommendations for individuals in terms of enhanced hygiene and keeping 1 to 2 metre social or in fact physical distance, or the government or local authority enforced restrictions for staying and working at home in self-quarantine, requirement to wear face mask in public places and transportation or even curfews, allowing gatherings with only a small number of people, lock-down of countries or districts by closing schools, universities and other public institutions as well as restaurants and shops, other than food markets, limiting public local, terrestrial and aerial transportation as well as non-essential entries to the countries or regions.

In addition, various countries have adopted comprehensive testing of even asymptomatic individuals together with tracking them with smart phone apps. It is evident that countries adopt, follow, and ease these restriction and confinement measures in a number of different ways and with different timings, as many of them tend to be strongly linked to the culture, politics, economy and overall well-being of the country. Furthermore, there are collective effects due to news and social media depending on how lethal the disease is perceived to be.

In order to make decisions of these large scale, and far reaching issues for mitigating the effects of the disease, one would need to quantify the results of restrictions on social contacting, cultural behaviour and habits, mobility, travelling and communication patterns of people. To realise this one needs to develop models that are able to make trustful predictions about the future behaviour of the disease in an interval of at least few months. These models should also take into account the pathological aspects of the virus, epidemiological factors including mechanisms of virus spreading, human behavioural, social, mobility, travelling and communication patterns, demographic factors including age, gender, and regional density of population as well as concentration in built environments, especially cities and public transportation volumes, terrestrially and aerially.

Over the past two decades a lot of effort and advance have been made to get understanding of the population level complex dynamics of infectious disease spreading [1–3]. In this, various epidemiological models have proved very versatile in implementing the above described epidemically relevant factors for qualitative and quantitative or predictive insight into the cause of infection spreading [4–7]. Models including geographical spread and population heterogeneity have also been developed [8–16], and recently, many models including different aspects of pandemics have been developed, see for example [17–20].

Here we present such a model, in which the biological aspects of the disease are combined with the social mechanisms of infection, related to population density and human mobility. The dynamical behaviour of the disease is modelled by considering a two dimensional grid of cells, weighted with the population density and by using a compartmental SEIRS (susceptible–exposed–infected–recovered–susceptible) in each cell. The geographical spread depends on the probability of infection associated with mobility parameters. Three kinds of mobility have been considered, namely short range terrestrial (between neighbouring cells), long range (between cells containing airports or train stations) and between randomly chosen cells, (simulating trips that people make without apparent reason). This model enables us to study not only the actual observed data, but also to predict the temporal evolution of the disease under hypothetical and changing scenarios of social distancing and confinement measures in a given geographical region. To do this and test the applicability of our model we perform a comparative study of three culturally and socioeconomically different countries: Mexico, Finland and Iceland. These countries differ not only in population size and density, but also in their behavioural habits, restriction and confinement policies, testing and tracking as well as how individuals follow and respond to them and to authorities.

This paper is organised such that after this Introduction (Section 1) we describe in Section 2 our model including the epidemiological microdynamics in each geographical cell and geographical macrodynamics between the cells. This is followed in Section 3 by the application of our model to three different countries by taking into account their characteristic data and the national restrictive interventions and their timings in each one of them.

2. Model

2.1. SEIRS epidemiological model (Microdynamics)

The model used in this study is based on the one presented earlier by Barrio et al. [12]. As depicted in Fig. 1, it considers the geographical spreading of the epidemics at two levels: the local dynamics and more global transmission of the disease from one geographical place to another. For this purpose, a two-dimensional grid of a country or region is constructed in such a way that within each cell (i, j) the population density $\rho(i, j)$ is considered to be homogeneous. For the local dynamics SEIR(S) model [21] is used for each cell, consisting of four compartments: not infected susceptible (X), exposed yet not infectious (E), infectious (Y), and recovered, temporarily immune (Z), representing an instantaneous local average state of the population.

In the model the periods of latency (ϵ), infectiousness (σ) and immunity (ω) are assumed to be constant and dimensionless by expressing them in units of a time scale τ of one day. Here we assume that the population size does

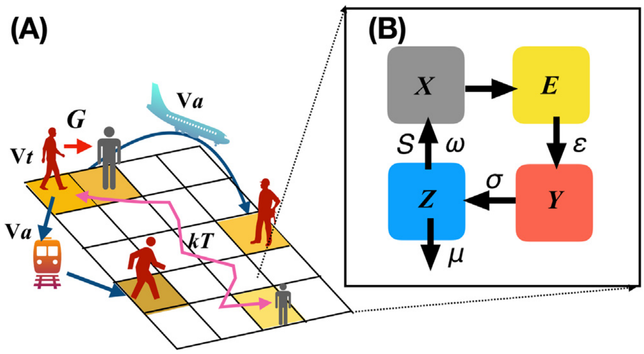

Fig. 1. (A) Schematic illustration of the model of epidemic spreading over a geographical region described as a two-dimensional grid of cells each with a given population density. The disease spreading takes place with two different mechanisms: the local dynamics within each cell by compartmental SEIRS model (B) and more global transmission from one geographical place to another describing the mobility of an individual (red: infected and grey: susceptible not yet infected) from one randomly chosen cell to another using different means of transportation.

not change throughout the simulation, i.e. $N = X + E + Y + Z = constant$ and for the mortality we assume an exponential functional form with a constant rate $\mu = 1/L$, where L is the life expectancy. The birth rate is μN with all the newborn considered susceptible. As people who have recovered do not necessarily become susceptible again, either because they die, or because of long lasting immunity or changes in social behaviour, the actual fraction of population that becomes susceptible (S) is included.

With all these assumptions, we can now express the flow rates per day for all the variables by the following map equations on each cell $\alpha = (i, j)$:

$$
\begin{aligned}
X_{t+1}(\alpha) &= q\left[X_t(\alpha) - G_t(\alpha) + Sq^b G_{t-1-b}(\alpha)\right] + \mu N,\\
E_{t+1}(\alpha) &= q\left[E_t(\alpha) + G_t(\alpha) - q^\epsilon G_{t-1-\epsilon}(\alpha)\right],\\
Y_{t+1}(\alpha) &= q\left[Y_t(\alpha) + q^\epsilon G_{t-1-\epsilon}(\alpha) - q^a G_{t-1-a}(\alpha)\right],\\
Z_{t+1}(\alpha) &= q\left[Z_t(\alpha) + q^a G_{t-1-a}(\alpha) - q^b G_{t-1-b}(\alpha)\right],
\end{aligned}
\tag{1}
$$

where $q = (1-\mu)$, $a = (\epsilon + \sigma)$, and $b = (\epsilon + \sigma + \omega)$. Unlike in case of other SEIRS models, in our model the probability of becoming infectious is not based on the mass action principle, but instead we use a biologically more sensible incidence function: $G_t(\alpha) = \rho(\alpha)X_t(\alpha)[1-\exp^{-\beta Y_t(\alpha)}]$, where β is a dimensionless constant representing the transmission parameter. As explained in [21], this expression generalises the mass action law to non-diluted cases where multiple interactions can be possible. In Fig. 1(B) this local model in each cell is represented, indicating the delay times in each step of the flow.

The model exhibits a rich variety of behaviour, as expected: regular oscillations of different period, damped oscillations, quasi-periodicity, chaos and stable regimes [21]. Therefore, the dynamics of other infectious diseases can be modelled with the same system, since all parameters so far, except the population density, characterise the disease, such as its virulence and lethality.

In this study we shall give specific values to these parameters to simulate the COVID-19 disease, and vary the social and demographic parameters when applied to the specific country or region, as discussed below.

2.2. Geographical disease spreading (Macrodynamics)

The relative population is represented by the values $\rho(\alpha)$ in the cells of a population matrix. The size of each cell is determined by the actual conditions of the country or region to be simulated. The model represents an instantaneous local average state of each cell and the disease can be transmitted from one cell to a contiguous cell because people move routinely, to work, shopping, etc., over distances slightly larger than the cell size. Therefore, the size of each cell should be congruent with the average distance that a person travels every day. In the case of the countries considered here this cell size is of the order of 7 km^2.

As illustrated in Fig. 1 we consider three mobility mechanisms:

1. Transmission of infection between neighbouring cells. This is often modelled as a diffusion process, but this implies that the susceptible one gets infected by certain amount, and the infectious one becomes healthier by the same amount. Instead of diffusion we take an alternative approach by describing the short distance transmission taking place with the average terrestrial mobility or velocity, v_t, which we assume to be stochastic in nature. Therefore, we can model the probability of spreading the disease from one cell to a neighbouring cell by using a Metropolis Monte-Carlo algorithm. First, one locates the potential spreader cells, this means having $Y_t(\alpha) \geq \eta$, where η is related to the infectiousness of the disease. Then, one chooses a random number from a uniform distribution ($p \in [0, 1]$), and

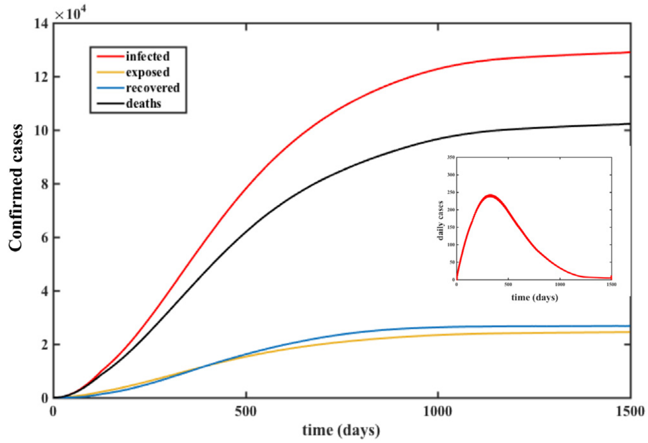

Fig. 2. Numerical simulation of the model showing the time history of the variables in a region of 506 × 737 cells with constant population density and unitary mobility parameters. In the inset the daily cases are shown.

if p is smaller than v_t, a neighbouring cell (denoted by α) becomes infected, that is $X(\alpha) = 1 - \eta$ and $Y(\alpha) = \eta$. We know very little about the real meaning of v_t, since the reasons for people to making a trip are quite varied. In this sense, v_t is related to the social and cultural habits of the individuals, and it is related to the average number of personal contacts per day.

2. Next we turn our attention to the influence of long distance travelling from one city to another by air or train on the disease spreading [20,22–27]. This process of transmission from a cell to another more distant cell we also assume to be stochastic. In this case, the probability of spreading the disease is proportional to the number of passengers per day travelling from one airport or station of a city to an airport or station of another city. This is simulated by locating the airports or stations in the grid and defining the long distance mobility parameter v_a. The probability of infection is represented by a weighted adjacency matrix (A) of the airline or transportation network, whose elements represent the average number of passengers between linked airports or train stations. Then, we run once again the Metropolis Monte-Carlo algorithm by using v_a to decide infectiousness between the elements of A (cells including the long range connections).
3. Since people occasionally make non-routine trips to distant towns, regardless of their population, we will assume noise to the transmission process. This will cause the spread of the epidemics to unexpected places. In order to simulate this we introduce a Monte-Carlo procedure, similar to the geographical spread of the illness. Therefore, we consider cells (α) in which there are not many susceptible individuals ($X_t(\alpha) < \eta$), at random, and compare the value of a random number p_0 with a quantity of the form $e^{-1/kT}$, since these random displacements can be considered analogous to the "kinetic energy" kT or "temperature" T of the system. If the Monte Carlo condition is fulfilled, then one starts the disease in that cell.

As an example of the kind of results obtained with this dynamics, we show in Fig. 2 the time history of the variables for a simulation in a two dimensional grid of 506 × 737 cells with constant population density of 1 for all the cells and unitary constant mobility parameters. The time parameters of the disease are hypothetical. As the initial condition we start infections simultaneously in 50 randomly chosen cells.

3. Application to the COVID-19 epidemics in Mexico, Finland and Iceland

As in this model the biological parameters are clearly separated from those related to social, cultural, and economic phenomena, one could adjust the biological parameters according to present knowledge. For the COVID-19 the latency, ϵ, is thought to be from 2 to 14 [19,28] days, though interestingly, $\epsilon = 1$ improved the adjustment of the data; the infectiousness $\sigma = 14$ is set to the standard "quarantine" time used in many countries; the immunity ω is yet unknown, but for another coronavirus, SARS-CoV, antibodies and memory T-cell response were detected 1 year or even longer after the infection [29,30].

To be conservative, here we use $\omega = 140$. Currently there are no data about the transmission parameter β and the disease infectiousness parameter η, so we estimated them to be $\beta = 0.91$ and $\eta = 0.1$, by adjusting Mexican data from March 2020. As we assume these parameters to be dependent on the specific virus and the immune response of its host, in this case COVID-19, we use them unchanged for the three countries studied here. However, the mobility parameters were adjusted for each country taking into account different social habits, strategies and measures used in them to mitigate the effect of the pandemic.

In all the following calculations the initial conditions were $X_{t=0} = 1$, $Y_{t=0} = E_{t=0} = Z_{t=0} = 0$ for all the cells and $X_{t=0}(\alpha) = 1 - \eta$ and $Y_{t=0}(\alpha) = \eta$, in the cells (α) where the first cases appeared.

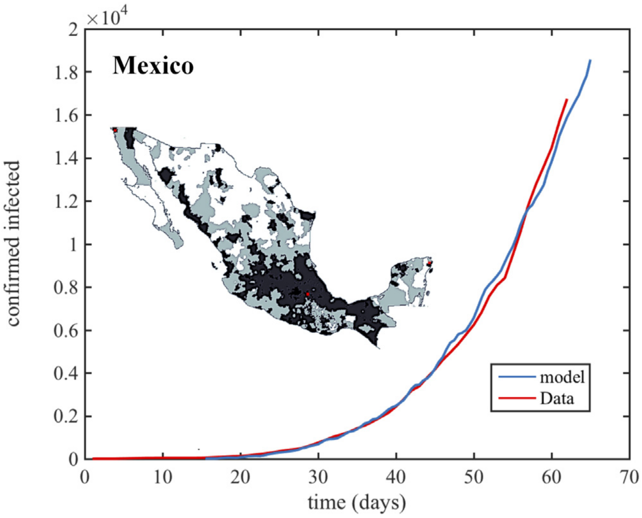

Fig. 3. Fitting the model parameters for the case of Mexico to actual data made on April 20th 2020. The exponential growth was reproduced for a set of mobility parameters that remain unchanged since the restrictions were imposed very early in March. February 28th is when the first case was reported and day zero is March 3rd. We show the map used which contains 372922 cells (cell size 7 km^2). The colours indicate the population density, ranging from more than 1000 people/km^2 (black) to less than 5 people/km^2 (light grey).

3.1. The case of Mexico

In order to illustrate the results obtained from the model, we use the geographical demographic data of Mexico from INEGI [31] and apply it to the outbreak of COVID-19 in 2020. The frequency of air travel and the number of passengers per day in Mexico were obtained from Dirección General de Aeronáutica Civil of the Secretaría de Comunicaciones y Transportes [32].

In Mexico the first imported case occurred in Mexico City (central Mexico) on the 28th of February 2020, and shortly after two more imported cases were reported, one in Mexico City and the other one in Sinaloa (northern Mexico). Mexican government together with Ministry of Health (Secretaría de Salud) implemented some measures such as tracking COVID-19 positive people and their contacts. On March 14th, the Ministry of Public Education (Secretaría de Educación Pública) extended Easter holidays in primary and high schools until April 20th in the whole country; some days later this period was extended until April 30th. On March 18th university students were sent home and social distancing was initiated. On March 23th, at national level, universities were closed as well as public places such as concerts, theatres, cinemas, churches, museums, gyms, zoos, and bars; home confinement was recommended. Airports were not closed, but they diminished their operations to only a small percentage of flights and passenger volumes. On March 26th non-essential activities of the government were suspended, and on March 30th non-essential economic activities at national level were suspended until May 30th (M1 in Fig. 4).

We made a calculation adjusting the mobility parameters to the data available from the John Hopkins University page [33]. The values which best fitted the data were: $v_t = 0.1$, $v_a = 0.02$, and $kT = 0.8$. These values represent an overall mobility reduction of approximately 65% of the normal values. There is also the possibility that the survival parameter S changes in time, if there were tests to detect potentially infected people and isolate them, or if there were vaccines, or effective medication in the near future. Until the first days of December 2020 this has not happened. So far this has not happened, so we used $S = 0.9$, throughout the calculations.

In Fig. 3 we show the fitting of the model to the actual data from march 1st to April 13th, averaged over 7 days. The actual data show an exponential increase of daily reported cases, so we fit the curve to a function of the form $a + be^{ct}$, where a is an expected shift in the number of reported cases, b is a scaling factor to adjust the actual number of reported cases and c is the growth exponent.

On May 25th the Mexican authorities announced a plan to lift the restrictions gradually, and asynchronously, considering the situation of the pandemic in each state. Consequently, the three mobility parameters and the frequency of flights would change with time slowly, from May to August assuming that the mobility will be restored to 50% of the value before the outbreak. Numerical predictions for a year were performed with two conditions, namely without lifting the restrictions, and following the plan to restore normality. We observed that the effect of lifting the restrictions is small but noticeable: the peak is attained around the 19th of July in both cases, but it was larger when restrictions were lifted, and then the epidemic would die off faster than in the case of doing nothing. However, the number of infected people would remain practically the same.

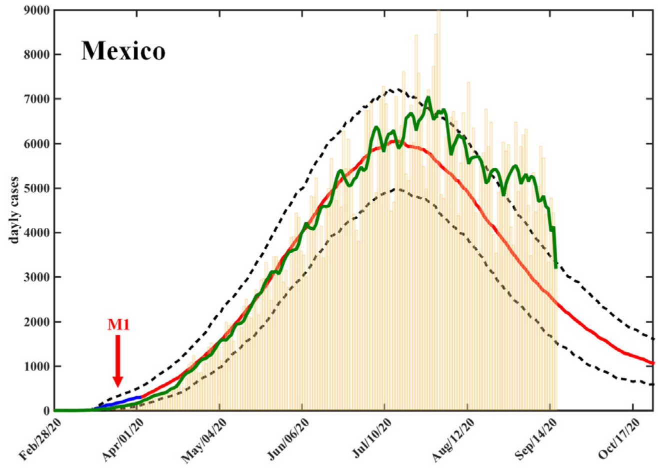

Fig. 4. Time history of the number of new cases per day in Mexico. Continuous blue line: daily confirmed cases from February 28th to April 13th used to adjust the model parameters. Continuous red line: numerical prediction assuming no further changes in societal conditions. Red arrow signals addition of restrictions. Broken black lines : 95% confidence interval. Bars: actual daily data up to September 15th. Green line is the 7-day average of the actual data.

In Fig. 4 we show an average of 50 realisations of the time history of the pandemic and it is seen to model very closely the actual data. This means that although costly economically, the social distancing measures are extremely effective in mitigating the effects of epidemics. It is remarkable that the prediction made in April holds tightly within the 95% confidence interval for **five** months. A maximum of the number of cases was predicted in April to occur between the 9th and the 19th of July, which actually was accurately realised.

3.2. The case of Finland

On January 29th 2020 Finland confirmed its first COVID-19 case. On February 26th and 28th, a second and third case were confirmed, which the National Institute of Health and Well being (THL) marked as the beginning of COVID-19 epidemic in Finland and from thereon reported the number of new cases [34] and advised the Finnish Government of its confinement measures. [35] On March 12th the Government decided on recommendations to curb the spread of corona virus by public events and workplaces closures, followed on March 16 by a lockdown of all schools and most government-run public facilities (theatres, libraries, museums etc.). In addition, at most 10 people were allowed to participate in public meetings, outsiders were forbidden from entering healthcare facilities and hospitals, and travel cross the internal Schengen and EU borders were limited to essential goods transportation and people having to because of work as well as citizens returning to Finland. These measures were scheduled to be in place until April 13th and later extended to May 13th at which point the pre- and primary schools were opened for the last two weeks of the spring semester, while other measures were kept in effect.

On March 27th, the Parliament voted unanimously to temporarily close the borders of the Uusimaa region (area surrounding the capital Helsinki), due to having most confirmed cases. On April 15th travel restrictions between Uusimaa region and the rest of the country were lifted. In addition, from April 4th to May 31st the Government decided to close all restaurants and hotels. From June 1st the gradual opening of the country started by opening restaurants, allowing the maximum number of people to be 50, public places such as museums and sports events all "with special arrangements" to maintain sufficient physical or social distance. On June 15th the Government lifted the restriction for travellers from Baltic and Nordic countries except Sweden to stay quarantined for 14 days, but kept intact the other international travel restrictions. These latter restrictions were lifted for July and part of August for a number of European countries and some Asian countries showing low number of cases but were reinstated again when these numbers started to show increase and signs of the second wave of the epidemic. From August 1st onward Government decided that the outdoor events with more than 500 people will be allowed with the arrangements to keep sufficient physical distance.

It is worth mentioning that for the summer 2020 people followed the confinement measures, restriction and recommendations by the Government quite closely, which caused a reduction of reported daily infection cases to less than 10. Mid August the primary and secondary schools were started and the Government recommended people wearing face masks in public transportation and places and continue to work remotely, if possible. In August the number of cases in Finland started to increase as signs of the second wave of the epidemic, which was then amplified in September as the universities and vocational schools started their autumn term. While the number of infections kept increasing mainly among younger people, October 1st the Government implemented the restriction for the restaurants and night-clubs to close latest by midnight and stop serving one hour before. As the number of infections kept increasing, mainly in the

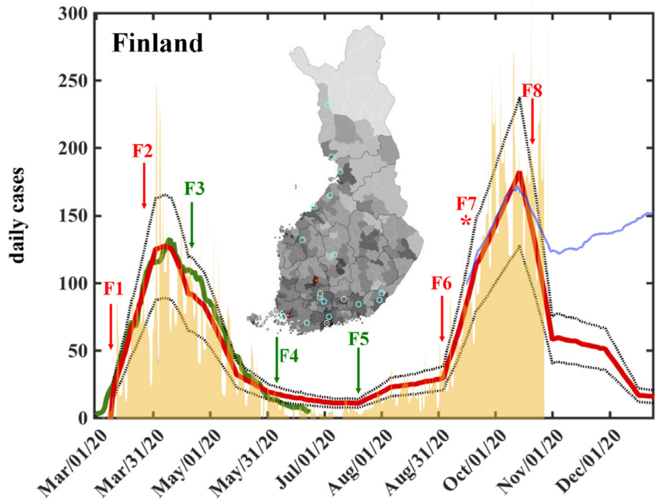

Fig. 5. Time history of the number of new cases per day in Finland. Average over 40 realisations of the model calculations (red line) showing the of 95% confidence interval (black broken lines) and the averaged data in green. Red arrows — addition of restrictions; green arrows — lifting restrictions; asterisk — super-spreader event The map used contains 248412 cells (cell size 2.7 km^2) and the population density colour code ranges from $>$ 1000 persons/km^2 (black) to $<$ 1 person/km^2 (light grey).

metropolitan region of Helsinki, all the gatherings larger than 20 people were banned from November 23rd till at least mid December.

Due to the above mentioned travel restrictions air travel reduced to 2%–3% from mid-March to May and to 6%–7% in June in comparison to the same months of the previous year (2019). In July the air travel volumes increased slightly to about 10% of the same time of the previous year and stayed at that level for August, September, and October. Due to strong recommendation by the Government to avoid travelling within Finland during mid-March to June period even the passenger volumes by railways were running low, but started picking up from mid-June on as people preferred having their vacations in Finland. The travel volumes were estimated to be only about 20% the value before the epidemic. Past the vacation period and for the autumn the travel volumes by railways reduced to about half of that of the previous year. Taking these measures into account we introduced them in the model to modify the aerial, terrestrial and casual or random mobilities along the time line of their introduction.

In order to investigate with our model the first wave of the epidemic, i.e. from March 1st to end of June 2020, we took notice of four major events: (i) the 12–14 March closing down (with v_t, reduced to 50%, $kT = 0.4$ (F1 in Fig. 5)), (ii) the March 27th isolation of the Uusimaa region (causing drastic reduction of v_t to 25% and $kT = 0.1$ (F2), (iii) the April 15th lifting travel restrictions of the Uusimaa region (with v_t and kT restored to the March values (F3)), and (iv) the air travel reduction from March to June, (with v_a changing from 2% in March–May to 7% in June (F4)).

The changes in mobility included for the simulations of the second wave were: a gradual removal of restrictions, including opening bars, schools and sport venues from July 23rd (F5) to September 3rd (F6), a super-spread event around September 11th (F7) and a severe reduction in mobility due to the recommendations of October 15th (F8). By taking into account all the above described measures till the end of October, we have performed a set of forty realisations and averaged them to calculate the 95% confidence interval of the model predictions. The results in Fig. 5 shows the average daily cases as a red line. Here it can be seen that our model predicts, from August onward, a slight increase in the number of daily cases, thus hinting the beginning of the second wave, and its rise to a larger number of daily cases than during the first wave, which actually appeared in September.

Thus our model turned out to be able to reproduce the overall behaviour and the two waves of the epidemic from the beginning of March 2020 till about the end of October 2020, surprisingly well. Beyond that date, and keeping the parameters fixed, our model shows a descending tendency for November and December as long as restrictions are maintained. In addition we show (in blue) a possible future scenario, assuming that the severe reduction in mobility due to the recommendations of October did not take place. In this case, the number of daily cases would continue at high levels, with a slight upward tendency, which could even lead to a higher incidence level. Indeed, this has happened but not because of lifting up the restrictive recommendation but because of the appearance of new more infectious variant of the corona virus.

3.3. The case of Iceland

On January 29th 2020, the countries Chief Epidemiologist advised against unnecessary travel to China, and recommended that people travelling from China undertake 14 days quarantine upon returning to Iceland. On the 31st of January,

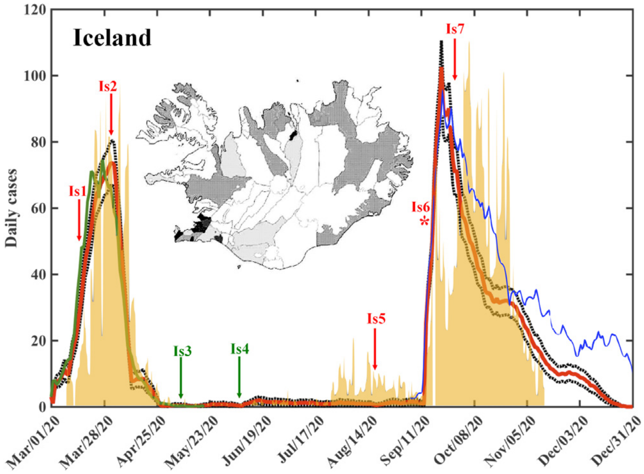

Fig. 6. Time history of the number of new cases per day in Iceland. Continuous green line: Actual data averaged over 7 days. Continuous red line: numerical prediction averaged over 20 realisations including the changes in social distancing mentioned in the text. The blue line is a single realisation assuming that the restrictions announced for Oct 5th were not implemented. Bars: actual data taken from [33]. Red arrows — addition of restrictions; green arrows — lifting restrictions; asterisk — super-spreader event. The map used contains 177,786 cells (cell size 1.4 km^2) and the population density colour code ranges from > 1000persons/km^2 (black) to < 1person/km^2 (light grey).

a meeting in the National Security Council was scheduled with the Minister of Health and Chief Epidemiologist. The Department of Civil Protection and Emergency Management (DCPEM) evoked the National Crisis Co-ordination Center. By the 3rd of February, Iceland had defined high-risk areas, including Northern Italy and Tirol, earlier than other governments, taking stricter measures with a 14-day quarantine requirement for all residents returning from those areas.

February 27th saw the first daily press conference, attended by Iceland's Chief Epidemiologist, Director of Health and Chief Superintendent. The first case of COVID-19 was confirmed in Iceland on February 28th. This was a person arriving from Northern Italy. DCPEM declared the alert phase. By March 6th over 30 imported cases had been confirmed and the first two transmissions within Iceland, traced to infected individuals who had recently travelled to Northern Italy. The alert level was raised to the emergency phase.

On March 13th, screening for the virus that causes COVID-19 started among the general public. deCODE genetics graciously offered to test everyone in the country who wanted to be tested. At the same time, a ban on gatherings of more than 100 people was announced and then implemented on the 16th. High schools and Universities were closed, and operations of kindergartens and primary schools were limited.

By March 31st, Iceland had limited gatherings to 20 people or fewer, closed sports clubs, hair salons, bars, and similar establishments, implemented fines for breaching the rules of quarantine, and became a party to an international contract which enabled the Icelandic authorities to join European Union members in the procurement of various healthcare equipment. April 2nd saw the tracing app Rakning C-19 become available in the App Store and Google Play to track the virus.

As a result of the quick action taken by the government, results from initial screenings indicated a low rate of infections among the general public. By April 21st, it was announced that the ban on gatherings and school activities would be relaxed, effective on May 4th 2020. The limit on the number of people who may gather increased from 20 to 50; pre-schools and primary schools reopened; athletic and youth activities became unrestricted again. On May 25th, gyms and swimming pools reopened and operated with limitations, such as a maximum number of guests. Gatherings of up to 200 people were allowed. All restaurants and bars re-opened with a curfew of 11 PM [36].

Taking these measures into account in the model we changed only the mobility parameters on the dates mentioned. We considered domestic flights operating with very few and diminishing number of passengers from the beginning of the outbreak, while the international airport was getting many imported cases until March 16th, when the aerial and terrestrial mobility were assumed to be reduced by 70% (Is1 in Fig. 6), reflecting the full obedience of the population to the confinement measures taken. Between April 2nd and April 9th a 90% mobility reduction was achieved (Is2), but on May 5th the mobility increased to 60% (Is3). The random mobility was kept to the original value of $kT = 0.8$, because of the uneven population density in the island, as 62% of the population is concentrated around the Reykjavik area, so it makes little difference if kT is reduced. We assume that one should expect around 1.5 cases per 1000 passenger coming from abroad.

In Fig. 6 we show the average over 20 realisation of the model and compare it with the actual data, both averaged over 7 days. We could say that in this case, the disease had been controlled in the early days of May. Our model simulates satisfactorily this first wave and the very low number of cases from May to August.

The borders opened on June 15th (Is4). Passengers arriving in the country were given the option of taking a COVID-19 test or undergoing quarantine for 14 days. Children born in 2005 and later were exempt. Testing was offered at Keflavík Airport and at other international ports of entry. Passengers were also required to answer a pre-arrival questionnaire, abide by sickness rules and were encouraged to download the app, Rakning C-19. At the same time, further relaxation of the ban on assembly took effect. The number of gatherings increased from 200 to 500 and restrictions on the number of swimming pools and fitness centres were reduced.

The results are encouraging, When adapting the model to a region with low population the stochasticity has more influence on the results, and it is more difficult to adjust the parameters in the case of Iceland. Despite the small number of cases predicted when opening the airport June 15th, the people of Iceland received a warning. As a result from imported cases, the number of local cases started to increase in late July into the beginning of August. Restricted measures were introduced at the border August 19th (Is5). This small wave seemed to be levelling off in mid-September. However, a local superspreading event introduced the beginning of a third wave (Is6), larger than the first one. The virus gained a stronghold in Iceland with more superspreading events. It seems that with further restrictions, such as encouraging work from home, ban on public events and gatherings of no more than ten people, in late October and beginning of November (Is7), have worked, so that after the third week in November the wave was clearly seen to be going down.

Considering these changes of the social compliance to distancing measures, we were able to simulate the second wave observed in September. Our model predicts very few cases by the end of December if constraints are maintained. We also performed a single calculation assuming that the restrictions on October 5th were not implemented to try predicting the effects that would result from these actions. In Fig. 6 we show this calculation in blue. Although the incidence declines toward December, the number of total cases will be larger.

4. Discussion and conclusions

Here we have presented a stochastic model of geographical spreading of infectious disease that differs in many respects from other compartmental SEIRS type models, commonly used to describe epidemic spreading. In particular, our model distinguishes the disease-defining epidemiological parameters from the ones that have to do with geography, and people's social habits and behaviour. The latter affect their mobility through societal traffic, travelling infrastructure and passenger flow networks based on roads, trains and airline routes. These mobility quantities could vary in time, in order to take into account the measures limiting them and to make predictions of future scenarios of the epidemic.

The recent review [37] discusses various approaches to model the COVID-19 pandemic in particular and it concludes that in order to the model to be predictive, a lot of precise data is needed. The fact that with our model presented here and with small amount of information we can make quite accurate predictions is due to our model seemingly catching up the intrinsic random nature of viral spreading. This model has performed well also with other viral diseases, as shown earlier in case of the swine influenza [12]. With the present study we have demonstrated that our model can be used for very different scales of population and their densities as well as for countries with different social structures and situations. Notice that the model was able to trace pandemic dynamics in Mexico, which is a big country having many local epidemics breaking out at different times in different federal states, as well as in Iceland which is an island with very low population.

By studying these three socially different countries we are able to learn several important lessons. First, it seems that it could be unwise to lift the country or regional level confinement measures, restrictions and recommendations completely, especially when the pandemic is still active in other regions where possible new strains of the virus could appear. This was well demonstrated in the case of Iceland and Finland. It shows that going back to a normality as free as last year will not be possible for a long time. Of course we hope that there is an effective vaccine, or treatment, available soon.

It should be noted that in the case of Mexico the model prediction of the behaviour of the pandemic was made early in the so called exponential phase, i.e. April 13th when the amount of available information was small, yet it has followed the actual number of cases very closely for five months.

We would like to emphasise that, unlike most compartmental models, our model is able to predict the appearance of a second wave (or even more waves) and its behaviour is closely related to the changes on the values of the mobility parameters. However, this holds only if the model parameters can be assumed not to change during the epidemic. Furthermore, new waves could be due to the appearance of new strains of the virus, which certainly modify the parameters modelling the disease. In the case a new variant that is more contagious and spreads more easily, we expect the emergence of new waves, even larger than the former ones.

Perhaps one of the most important points of this comparative study is that the timely social distancing and confinement measures, as well as public recommendations and restrictions are seemingly efficient ways to control the disease spreading, especially when people follow them tightly, as it seemed to be the case for the first half a year of the pandemic in Finland and Iceland, both being sparsely populated and socially relatively homogeneous countries. In addition, in case of Iceland from the very beginning of the epidemic the population-wide testing and tracking served as an enhanced control and life-saver. In case of Mexico imposing confinement measures is more complicated, because of much larger population and very large densely populated cities with huge socioeconomic differences. Still the authorities have managed to slow down the speed of disease spreading. The price to pay in all these three countries is that the pandemic could stay active for quite a while, but on the other hand our understanding of confinement and prevention measures, i.e. non-pharmaceutical interventions, have proven their efficiency.

In this publication our model is updated to November 20th 2020, when it was first submitted to this journal. Since then it has been extended to consider tracking and isolating asymptomatic individuals [38], and also to take into account vaccinations and related strategies for mitigating the pandemic [39], and at the moment we are applying it to study the emergence of new virus variants and their changed epidemiological properties. In these publications we can reproduce the new waves that have been seen during 2021.

CRediT authorship contribution statement

Rafael A. Barrio: Conceptualization, Methodology, Methods and calculations, Manuscript preparation, Reviewing of the present work. **Kimmo K. Kaski:** Conceptualization, Methodology, Methods and calculations, Manuscript preparation, Reviewing of the present work. **Guđmundur G. Haraldsson:** Conceptualization, Methodology, Methods and calculations, Manuscript preparation, Reviewing of the present work. **Thor Aspelund:** Conceptualization, Methodology, Methods and calculations, Manuscript preparation, Reviewing of the present work. **Tzipe Govezensky:** Conceptualization, Methodology, Methods and calculations, Manuscript preparation, Reviewing of the present work.

Declaration of competing interest

The authors declare that they have no known competing financial interests or personal relationships that could have appeared to influence the work reported in this paper.

Acknowledgements

RAB acknowledges support from The National Autonomous University of Mexico (UNAM) and Alianza UCMX of the University of California (UC), through the project included in the Special Call for Binational Collaborative Projects addressing COVID-19. RAB was financially supported by Conacyt, Mexico through project 283279. KK acknowledges support for Visiting Fellowship at The Alan Turing Institute, UK, and the European Community's H2020 Research Infrastructures "SoBigData++: Social Mining and Big Data Ecosystem" project.

References

[1] R.M. Anderson, R.M. May, Infectious Diseases of Human. Dynamics and Control, Oxford Univ. Press, Oxford, 1992.
[2] N. Bailey, The Mathematical Theory of Epidemics, Charles Griffin, London, 1957.
[3] Castillo-Chávez, A. Yakubo, Discrete time SIS models with simple and complex dynamics, in: C. Castillo-Chávez, S. Blower, P. van den Driessche, D. Kirshner, A. Yakubo (Eds.), Mathematical Approaches for Emerging and Reemerging Infectious Diseases. An Introduction, Springer-Verlag, 2002, pp. 153–163.
[4] A. Johansen, A simple model of recurrent epidemics, J. Theoret. Biol. 178 (1996) 45–51.
[5] W.P. London, J.A. Yorke, Recurrent outbreaks of measles, chickenpox and mumps: I. Seasonal variation in contact rates, Am. J. Epidemiol. 98 (1973) 453–468.
[6] M. Bootsma, N. Ferguson, The effect of public helth measures on the 1918 influenza pandemic in U.S. cities, Proc. Natl. Acad. Sci. USA 104 (2007) 7588–7593.
[7] C. Viboud, P.Y. Boëlle, K. Pakdaman, F. Carrat, A.J. Valleron, A. Flahault, Influenza epidemics in the United States, France, and Australia, 1972–1997, Emerg. Infect. Diseases 10 (2004) 32–39.
[8] I.M. Longini Jr., A. Nizam, S. Xu, K. Ungchusak, W. Hanshaoworakul, D.A.T. Cummings, M.E. Halloran, Containing pandemic influenza at the source, Science 309 (2005) 1083–1087.
[9] S. Cauchemez, A. Valleron, P. Boëlle, A. Flahault, N. Ferguson, Estimating the impact of school closure on influenza transmission from sentinel data, Nature 452 (2008) 750–755.
[10] D. Balcan, V. Colizza, B. Gonçalves, H. Hud, J.J. Ramascob, A. Vespignani, Multiscale mobility networks and the spatial spreading of infectious diseases, Proc. Natl. Acad. Sci. USA 106 (51) (2009) 21484–21489.
[11] F. Simini, M. González, A. Maritan, B. A.L., A universal model for mobility and migration patterns, Nature 484 (2012) 96–100.
[12] R. Barrio, C. Varea, T. Govezensky, M. José, Modeling the geographical spread of influenza A(H1N1): The case of Mexico, Appl. Math. Sci. 7(44) (2013) 2143–2176.
[13] A. Apolloni, C. Poletto, J. Ramasco, P. Jensen, C. V., Metapopulation epidemic models with heterogeneous mixing and travel behaviour, Theoret. Biol. Med. Model. 1:3 (2014) PubMed: 24418011.
[14] R. Marguta, A. Parisi, Impact of human mobility on the periodicities and mechanisms underlying measles dynamics, J. R. Soc. Interface 12 (2015) PubMed: 25673302.
[15] E. Santermans, E. Robesyn, T. Ganyani, B. Sudre, C. Faes, C. Quinten, W. Van Bortel, T. Haber, T. Haber, F. Van Reeth, M. Testa, N. Hens, D. Plachouras, Spatiotemporal evolution of ebola virus disease at sub-national level during the 2014 West Africa epidemic: Model scrutiny and data meagreness, PLoS One 11 (1) (2016) e0147172.
[16] G. Chowell, L. Sattenspiel, S. Bansal, C. Viboud, Mathematical models to characterize early epidemic growth: A review, Phys. Life Rev. 18 (2016) 66–97.
[17] X. Conghui, Y. Yongguang, C. YangQuan, L. Zhenzhen, Forecast analysis of the epidemics trend of COVID-19 in the united states by a generalized fractional-order SEIR model, Nonlinear Dyn. (2020) unpublished.
[18] L. Zhenzhen, Y. Yongguang, C. YangQuan, R. Guojian, X. Conghui, W. Shuhui, Y. Zhe, A fractional-order SEIHDR model for COVID-19 with inter-city networked coupling effects, ArXiv (2020) 12308v3.
[19] Y. Chayu, W. Jin, A mathematical model for the novel coronavirus epidemic in Wuhan, China, Math. Biosci. Eng. 17 (3) (2020) 2708–2724.
[20] S. Bekiros, D. Kouloumpou, A new mathematical model of infectious disease dynamics, Chaos Solitons Fractals 136 (2020) 109828.
[21] M. José, T. Govezensky, A. Lara Sagahon, C. Varea, R. Barrio, A discrete SEIRS model for pandemic periodic infectious diseases, Adv. Stud. Biol. 4 (2012) 153–174.

[22] R.F. Grais, J.H. Ellis, A. Kress, G.E. Glass, Modeling the spread of annual influenza epidemics in the U.S.: The potential role of air travel, Health Care Manag. Sci. 7 (2004) 127–134.
[23] J.H. Grais, G.E. Glass, Assessing the impact of airline travel on the geographic spread of pandemic influenza, Eur. J. Epidemiol. 18 (2003) 1065–1072.
[24] I.M. Longini Jr., P.E. Fine, S.B. Thacker, Predicting the global spread of new infectious agents., Am. J. Epidemiol. 123 (1986) 383–391.
[25] L. Rvachev, I.M. Longini Jr., A mathematical model for the global spread of influenza, Math. Biosci. 75 (1985) 3–22.
[26] A. Flahault, S. Deguen, A.J. Valleron, A mathematical model for the European spread of influenza, Eur. J. Epidemiol. 10 (1994) 471–474.
[27] J.S. Brownstein, C.J. Wolfe, K.D. Mand, Empirical evidence for the effect of airline travel on inter-regional influenza spread in the United States, PLoS Med. 3 (10) (2009) e401.
[28] C. Rothe, M. Schunk, P. Sothmann, G. Bretzel, G. Froeschl, C. Wallrauch, et al., Transmission of 2019-nCoV infection from an asymptomatic contact in Germany, N. Engl. J. Med. (2020).
[29] O. Janice, A. Ken-En, Y. Tan, Understanding the t cell immune response in SARS coronavirus infection, Emerg. Microbes Infect. 1(9) (2012) e23.
[30] O. Ng, A. Chia, A. Tan, R. Jadi, H. Leong, A. Bertoletti, Y. Tan, Responses targeting the SARS coronavirus persist up to 11 years post-infection, Vaccine 34 (17) (2016) 2008–2014.
[31] I.N. de Estadística y Geografía, 2020, https://www.inegi.org.mx.
[32] D.G. de Aeronáutica Civil of the Secretaría de Comunicaciones y Transportes, 2020, https://www.sct.gob.mx.
[33] J.H.U.J. map, 2020, https://coronavirus.jhu.edu/map.htm.
[34] F.I. of Wellfare, 2020, https://thl.fi/en/web/thlfi-en.
[35] Information and advice on the coronavirus, https://valtioneuvosto.fi/en/information-on-coronavirus.
[36] T.D. of Health, T.D. of Civil Protection, E. Management, 2020, https://www.covid.is/sub-categories/icelands-response (cited June 9), URL `Icelands response`.
[37] A. Vespignani, H. Tian, C. Dye, J.O. Lloyd-Smith, R.M. Eggo, M. Shrestha, S.V. Scarpino, B. Gutierrez, M.U.G. Kraemer, J. Wu, K. Leung, G.M. Leung, Modelling COVID-19, Nature Rev. 2 (2020) 279–281.
[38] N. Barreiro, T. Govezensky, P. Bolcatto, R. Barrio, Detecting infected asymptomatic cases in a stochastic model for spread of COVID-19: the case of Argentina, Sci. Rep. 11 (2021) 10024.
[39] N. Barreiro, C. Ventura, T. Govezensky, M. Núñez, P. Bolcatto, R. Barrio, Strategies for COVID-19 vaccination under a shortage scenario: a geo-stochastic modelling approach, 2021, arXiv:2104.09590.